Distance Measurement Based on Linear Phase Correlation in WiFi CSI

Qingfei Kang(✉), Liangbo Xie, Mu Zhou, and Zengshan Tian

School of Communication and Information Engineering,
Chongqing University of Posts and Telecommunications, Chongqing 400065, China
S160131065@stu.cqupt.edu.cn, {xielb,zhoumu,tianzs}@cqupt.edu.cn

Abstract. In this paper, we propose a new distance measurement algorithm based on WiFi Channel State Information (CSI). In order to resolve the phase error in traditional commodity WiFi devices, we design a system based on the Universal Software Radio Peripheral (USRP) with GNU Radio to analyze and separate the mixed phase errors. After the calibration of the CSI phase, it is found that the clock divider phase offset (DPO), which is introduced by the random phase offset in the clock, will affect the CSI phase, and a clustering-based method is proposed to remove the effect of DPO. We recover the linear relationships among the subcarriers phase and combine the center subcarrier phase to estimate the distance. In our algorithm, we can complete the distance measurement by using only one frequency band. Experiment results indicate that our algorithm can achieve centimeter-level accuracy in distance measurement.

Keywords: WiFi · CSI phase · GNU Radio · Distance measurement

1 Introduction

The Channel State Information (CSI) exposed by WiFi device, which is measured in channel equalization, is widely used for location as a replacement of Received Signal Strength Indication (RSSI). Due to the difficulty of eliminating CSI phase error, most of the recent WiFi location systems are based on the CSI amplitude as the substitution of RSSI. As we known, Chronos [1] is the first system to use CSI phase for location, however, Chronos only uses the zero-subcarrier to avoid the linear phase error and needs frequency hopping in the device. Splicer [2] combines amplitude with the phase in 10 different bands rather than only use the phase with mixed phase errors to locate the target but it also needs to frequency sweeping. What's more, in order to improve the positioning accuracy the above applications have focused on the distance measurement accuracy and the accuracy of phase plays an important role in distance measurement.

According to previous work [3], most methods conduct a linear transform on the raw CSI phase to remove the linear CSI phase errors, which move the mean

S. Han et al. (Eds.): AICON 2019, LNICST 286, pp. 167–174, 2019.
https://doi.org/10.1007/978-3-030-22968-9_15

of phases on all sub-carriers to zero. After the phase adjustment, the phase slope between the subcarriers, which includes the linear phase caused by the Time-of-Flight (ToF) is also forced to zero. As a result, the linear transform method can't use the phase difference between the subcarriers to estimate the ToF. Recent work [4] subtracts the linear slope value by conducting a linear fitting from the raw CSI phase. But the value can't be used to represent the slope caused by the ToF since the Sampling Frequency Offset (SFO) is mixed with ToF. To remove the SFO, high precise synchronization across the device is needed, SourceSync [5] implement a symbol level synchronizer WiFi system on the customized Field Programmable Gate Array (FPGA) platform, but such mechanisms are not available in the public. Hence, we use Universal Software Radio Peripheral (USRP) to do high precise synchronization, which has a variety of alternative method to synchronize different devices such as Multiple Input Multiple Output (MIMO) Cable and GPS Disciplined Oscillator (GPSDO) or external reference clock. What's more, by using the GNU Radio platform, we can develop our WiFi receiver quickly to collect the physical layer CSI information as we want.

Specifically, by using the synchronization feature of USRP, we can remove the main phase errors in CSI, but we find a new Divider Phase Offset (DPO) caused by the divider in USRP N210, which also exists on the commodity WiFi devices. To address this issue, we propose a strategy to eliminate the DPO and recover the linear phase slope between the subcarriers. After that, we use the accurate phase slope value and combine the zero-subcarrier phase to measure the distance.

The rest of this paper is organized as follows. We first make a overview of our system design in Sects. 2 and 3 describes the phase error calibration method in our system. We evaluate the performance of our system in Sect. 4 and we conclude in Sect. 5.

2 System Design

2.1 Signal Model

To simplify the channel model in [6], we only consider the environment with the single direct propagation path. The channel response $h(f)$ can be simplified as:

$$h(f) = \alpha \cdot e^{-j \cdot 2\pi \cdot f \cdot \tau}, \tag{1}$$

where α represents the amplification factor of amplitude and τ represents the propagation delay of the signal. Since the different subcarriers in the same frequency band undergo the same ToF, the phase difference $\Delta_{m,n}$ between subcarriers m and n can be expressed as:

$$\Delta_{m,n} = -2\pi \cdot (f_m - f_n) \cdot \tau \bmod 2\pi, \tag{2}$$

where f_m and f_n are the frequency of subcarriers m and n in the passband. We conduct that the phase ambiguity between two consecutive subcarriers only

occurs when the phase difference between two consecutive subcarriers greater than 2π. In our usual usage, the WiFi signal propagation delay is much smaller than this value. Under such a premise, we can describe Eq. (2) as:

$$\Delta_{m,n} = -2\pi \cdot (f_m - f_n) \cdot \tau, \tag{3}$$

From Eq. (3) we can observe an obvious linear relationship between the phase and subcarriers index after we transform Eq. (3) as:

$$\phi_m = \phi_0 - 2\pi \cdot k \cdot f_s \cdot \tau, \tag{4}$$

where ϕ_m is the phase of the mth subcarrier, k is the index of subcarriers, which ranges from 0 to 53. ϕ_0 represents the phase of the first subcarrier and the f_s is the frequency spacing between two consecutive subcarriers. In order to calculate the distance, we need to get the ToF, which can be obtained by fit the phase slope. In Eq. (4) τ is multiple with k, we take its partial respect to k and obtained the phase slope s:

$$s = -2\pi \cdot f_s \cdot \tau, \tag{5}$$

since the max resolution of the CSI slope that represent ToF is only limited to the sampling period T_s [7] and we take it to Eq. (5) as:

$$s = -2\pi \cdot f_s \cdot (\tau \bmod T_s)\,. \tag{6}$$

According to [1], the zero-subcarrier phase θ with the center frequency f_c can also represent ToF since it won't be affected by the linear phase error and can be express as:

$$\theta = -2\pi \cdot f_c \cdot \left(\tau \bmod \frac{1}{f_c}\right), \tag{7}$$

If we can get the CSI phase without any additional phase error, the slope s in Eq. (6) and the zero-subcarrier θ in Eq. (7) should have the relationship as the picture plotted in Fig. 1.

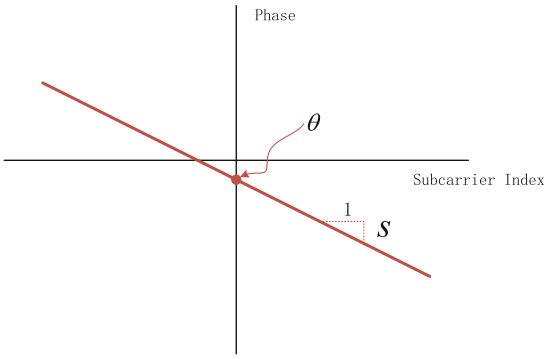

Fig. 1. The CSI phase without phase error in theoretically.

2.2 Distance Measurement

From Eqs. (6) and (7), both the zero-subcarrier phase and the phase slope have the ambiguity that can't represent the true ToF. Notice that the center frequency f_c, which defined in the standard should have the fixed value (e.g., 2.412 GHz, 2.417 GHz, 2.422 GHz, etc.). And the sampling period T_s is related to the bandwidth, which should have a value of 20M or 40M in normal usage. We note that T_s is not an integer multiple of $\frac{1}{f_c}$ and the above ambiguity can be resolved by the well-known Chinese remainder theorem [8]. We get the initial ambiguity value of phase slope s and zero-subcarrier θ and combine Eqs. (6) and (7) to search real ToF τ as described in Fig. 2.

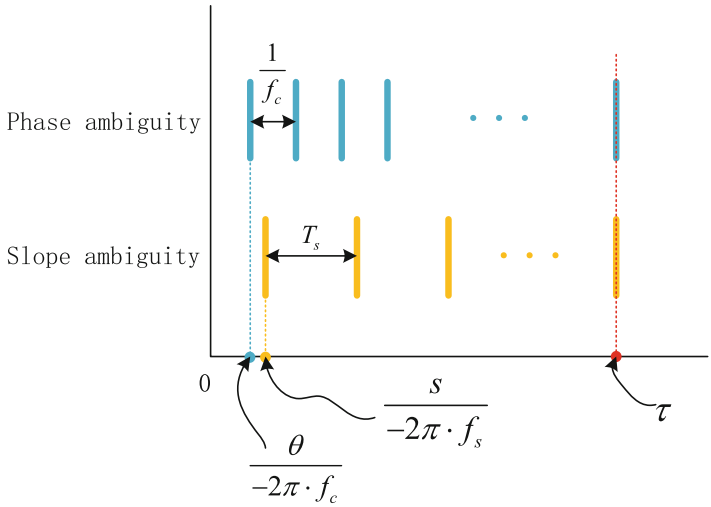

Fig. 2. Resolve phase ambiguity by phase slope and zero-subcarrier phase.

2.3 CSI Measurement Phase Error Source

Generally speaking, we can easily use the phase, which can be achieved from the CSI reported by the Network Interface Cards (NICs) to measure the distance. But previous studies have reported the CSI phase mixed with rich hardware distortions. Besides environment noise, previous researchs [6,9] have resolved the sources of CSI phase errors and we make a summary of the major phase error.

Carrier frequency offset (CFO). CFO exists since the mismatch of the crystal oscillator between the transmitter and the receiver that can't produce the consistent central frequencies. This frequency offset can be roughly removed in the stage of frequency synchronization. But residual frequency offset remain exists that will affect the CSI phase heavily.

Sampling frequency offset (SFO). SFO is a difference between the sampling clock of the Analog to Digital Converter (ADC) and the Digital to Analog Converter (DAC), which will cause a difference of sampling period. This error will gradually increase and lead to a rotation error. This rotation error will cause ambiguity in CSI phase that disrupts the linear relationship between subcarrier.

Divider Phase Offset (DPO). DPO is caused by the divider, which doesn't lock the output clock phase. Since any timing shift on the ADC clock is combined with the desired signal at the ADC output. For this reason, the DPO in ADC clock will introduce a phase error to the CSI phase. As we need a sample rate of 20 MHz, which divides from the 100 MHz master clock in USRP N210, we get 5 different slopes in the CSI phase. What's more, DPO also includes a phase offset like CFO if the ADC and frequency mixer use single clock source. As we can see from Fig. 3 the red line represents the phase without phase error, and one blue line represents one packet CSI phase, which mixed with CFO and SFO. If we collet lots of packets and the phase between two blue lines is DPO.

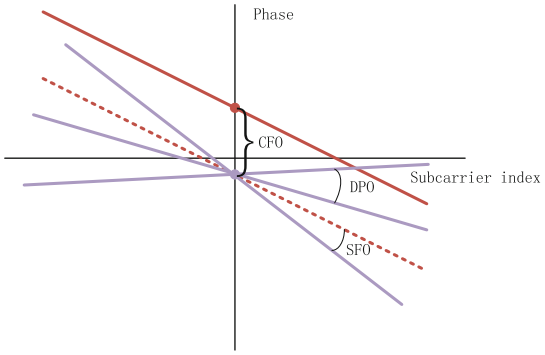

Fig. 3. The CSI phase with phase errors. (Color figure online)

3 Phase Error Calibration

As we known, CFO and SFO are caused by the crystal oscillator mismatch between the transmitter and the receiver. It can be easily resolved when we synchronize transmitter and receiver by using the fantastic feature of USRP. We test this method in USRP N210.

We first collect 50 packets CSI without any synchronization methods with the constant distance. And then we repeat the experiment again by using MIMO Cable for synchronization. We plot the unwrapped CSI phase in Fig. 4.

From Fig. 4(b) we can see the phase has an obvious linear relationship between the subcarrier index compare to Fig. 4(a) since the SFO is removed. And the phase of zero-subcarrier (27th subcarrier) become stable since the CFO is also removed once we synchronize two USRP devices.

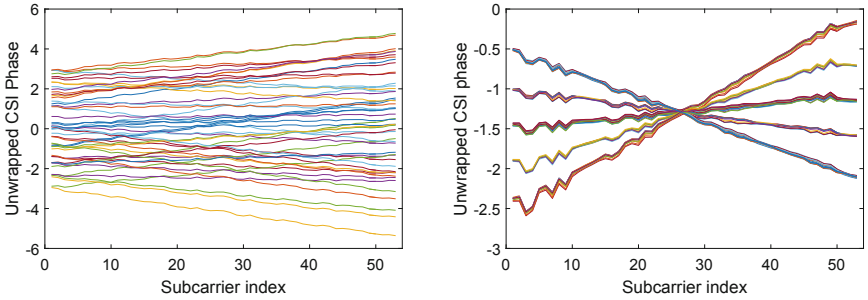

(a) Phase without synchronization (b) Phase with synchronization

Fig. 4. Effect of synchronization.

We note that DPO will lead to a rotation error, which has a fix rotation values in Fig. 4(b) and can be solved by clustering-based algorithm. We first get 5 different slopes by clustering the phase slopes. After that, we can select one slope to represent the true slope, which will include a ambiguity of $\frac{T_s}{div}$ in Eq. (6). *div* represents the divide ratio of the master clock, which is a constant. But this ambiguity can be also resolved by Chinese remainder theorem since it only reduces the period of s.

4 Performance Comparison

To verify our idea, we conduct a series of experiment in USRP with a spacious environment, which is the LOS environment without the multi-path distraction. We use N210 motherboard and UBX-40 daughter board as the transmitter and the receiver which be synchronized by MIMO Cable. In order to remove the DPO in frequency mixer, we can only use the center frequency is multiples of the master clock 100M, which means our experiments will limit the test distance to 3 m.

In order to use the zero-subcarrier for distance measurement, we need to get the stable zero-subcarrier phase. We conduct an experiment with the center frequency of 2.4 GHz and we restart the devices 20 times to collect 1000 packets. We find that the phase of zero-subcarrier is much stable with an error less than 0.15 rad, which means that the max error of distance calculated by the zero-subcarrier is less than 0.3 cm. This accuracy has met our requirements.

After we clustering the phase slope, we need to select one slope from 5 slopes to represent the ToF. In order to select the slope with minimal error, we calculate the variance of the 5 different slopes in Fig. 5(a) from the max slope to the min slope and plot the variance in Fig. 5(b). We can find that the minimal slope which plots in red color in Fig. 5(a) has the smallest variance. We repeat this experiment many times and come to the same conclusion. And we find the range of the minimal slope is about 0.00055, which means that the max error of distance calculated by the phase slope is less than 8.4 cm.

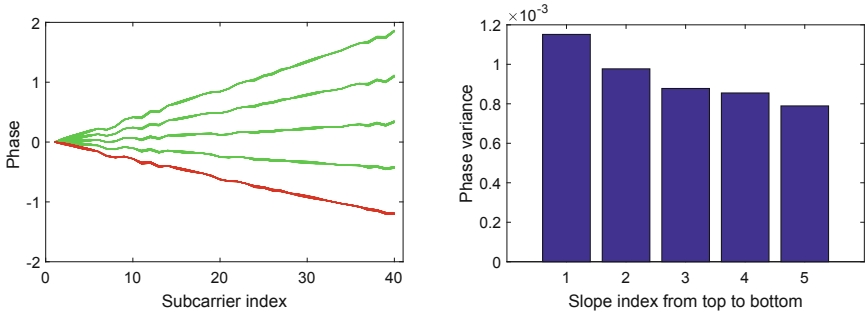

(a) The five slope caused by DPO (b) The variance of different slope

Fig. 5. Phase slope selection. (Color figure online)

To measure the distance, we fix the transmitter and move the receiver. For each distance, we collect 200 packets CSI. But we can only under the max distance of 3 m since the power of the signal is limited by the hardware. In Fig. 6, we provide detailed statistical results for performance achieved by the algorithm described in Sect. 2 with different distance.

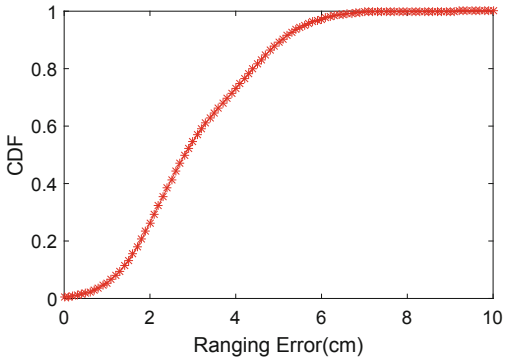

Fig. 6. Distance measurement result.

Compare to the max accuracy system that using WiFi signal [1], our system can achieve the distance error less than 10 cm by using the synchronization feature of USRP, which is superior to the best performance of 26 cm in Chronos.

5 Conclusion

This paper design a new distance measurement system. From the CSI collect by the USRP devices we analysis the mixed phase error in CSI phase and identify a

new divider phase Error. We use the synchronization feature of USRP to remove the differential phase error. After that, we use a clustering-based method to remove the DPO in ADC and recover the linear relationship between CSI phase and subcarrier index. At last, we propose an algorithm by using the linear phase combine the zero-subcarrier phase to estimate the distance in LOS and non-multipath environment. In our experiment, we can achieve 6 cm accuracy in distance tracking.

References

1. Vasisht, D., Kumar, S., Katabi, D.: Decimeter-level localization with a single WiFi access point. In: NSDI, vol. 16, pp. 165–178 (2016)
2. Xie, Y., Li, Z., Li, M.: Precise power delay profiling with commodity Wi-Fi. IEEE Trans. Mob. Comput. **18**(6), 1342–1355 (2018)
3. Wang, Y., Liu, J., Chen, Y., Gruteser, M., Yang, J., Liu, H.: E-eyes: device-free location-oriented activity identification using fine-grained wifi signatures. In: Proceedings of the 20th Annual International Conference on Mobile Computing and Networking, pp. 617–628. ACM (2014)
4. Kotaru, M., Joshi, K., Bharadia, D., Katti, S.: SpotFi: decimeter level localization using WiFi. In: ACM SIGCOMM Computer Communication Review, vol. 45, pp. 269–282. ACM (2015)
5. Rahul, H., Hassanieh, H., Katabi, D.: SourceSync: a distributed wireless architecture for exploiting sender diversity. ACM SIGCOMM Comput. Commun. Rev. **41**(4), 171–182 (2011)
6. Zhuo, Y., Zhu, H., Xue, H., Chang, S.: Perceiving accurate CSI phases with commodity WiFi devices. In: IEEE Conference on Computer Communications, INFOCOM 2017, pp. 1–9. IEEE (2017)
7. IEEE Working Group, et al.: IEEE standard for information technology-telecommunications and information exchange between systems-local and metropolitan area networks-specific requirements-part 11: wireless LAN medium access control (MAC) and physical layer (PHY) specifications amendment 6: wireless access in vehicular environments. IEEE Std 802(11) (2010)
8. Dingyi, P., Arto, S., Cunsheng, D.: Chinese Remainder Theorem: Applications in Computing, Coding, Cryptography. World Scientific, Singapore (1996)
9. Zhu, H., Zhuo, Y., Liu, Q., Chang, S.: π-splicer: Perceiving accurate CSI phases with commodity WiFi devices. IEEE Tran. Mob. Comput. **17**(9), 2155–2165 (2018)